



Supplementary Information for

**USP7 Regulates ALS-associated Proteotoxicity and
Quality Control Through the NEDD4L-SMAD Pathway**

Tao Zhang^{a,b,1}, Goran Periz^{a,b,1}, Yu-Ning Lu^{a,b}, Jiou Wang^{a,b,2}

Corresponding author: Jiou Wang

Email: jiouw@jhu.edu

This PDF file includes:

Supplementary Figures, Tables and Legends

Figure S1 to S8

Table S1 and S2

Supplementary Figure 1

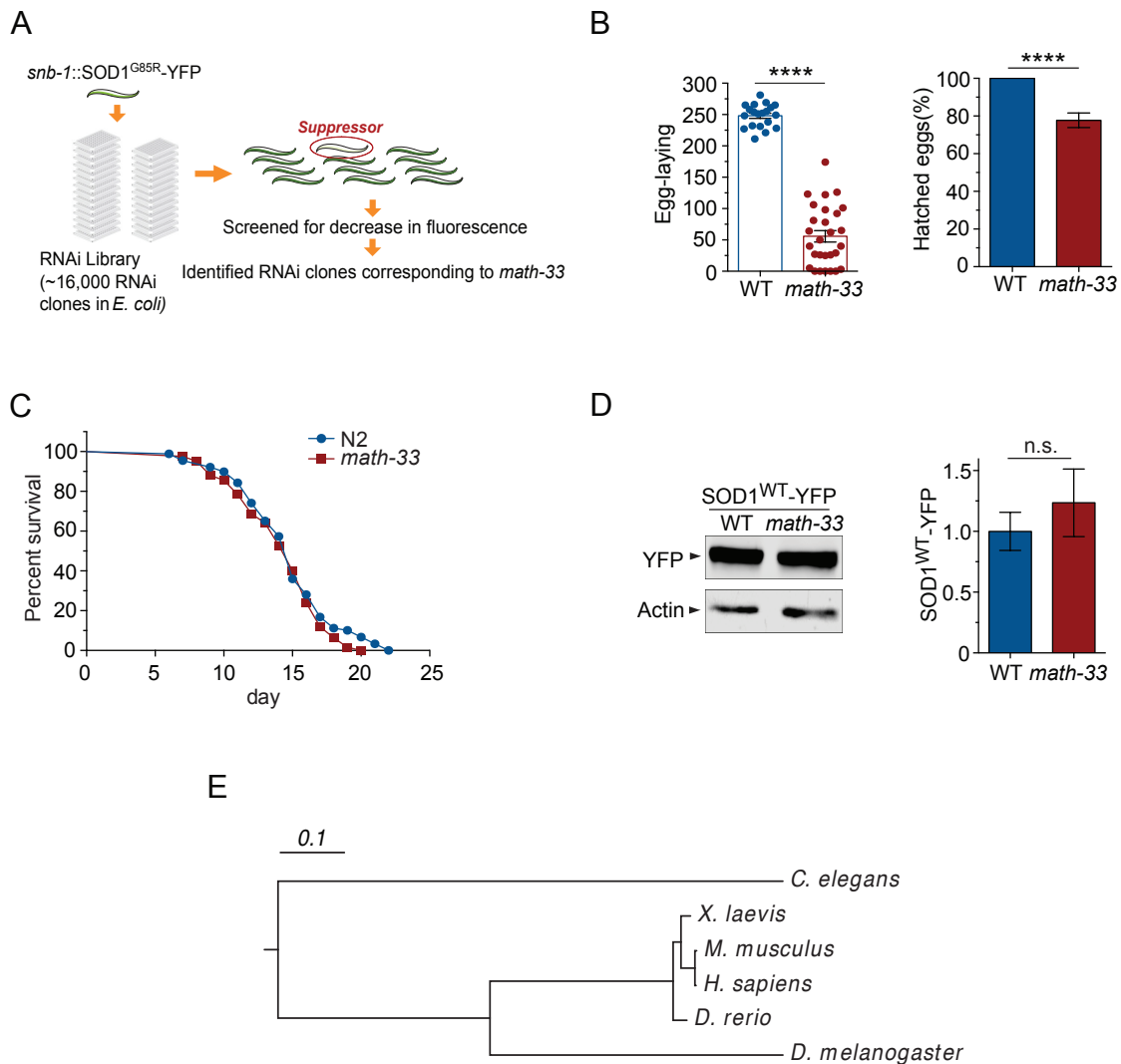


Fig. S1. The conserved function of USP7 as a regulator of proteotoxicity. (A) Scheme of the *C. elegans* RNAi screen that identified the gene whose knockdown reduced SOD1^{G85R}-YFP protein aggregation in neurons. (B) Brood sizes, as measured by counting the total numbers of eggs laid, of WT and *math-33(ok2974)* mutant worms (left) [N2, n=20; *math-33(ok2974)*, n=28; **** $p < 0.0001$]. The percentages of hatched eggs among the total eggs laid are shown (right) [N2, n=20 egg-laying animals; *math-33(ok2974)*, n=23 egg-laying animals; **** $p < 0.0001$]. (C) Longevity, as measured by surviving days, of WT and *math-33(ok2974)* mutant worms [N2,

n=89; *math-33(ok2974)*, n=125]. (D) Western blot analysis of proteins extracted from the WT and *math-33(ok2974)* mutant worms. Representative immunoblots of SOD1^{WT}-YFP (left) and quantification of SOD1^{WT}-YFP protein (right; n=3, n.s., non-significant) are shown. (E) Molecular phylogenetic analysis of MATH-33/USP7 homologs in different species. The tree is drawn to scale, with branch lengths indicative of relative evolutionary time. Error bars indicate \pm SEM.

Supplementary Figure 2

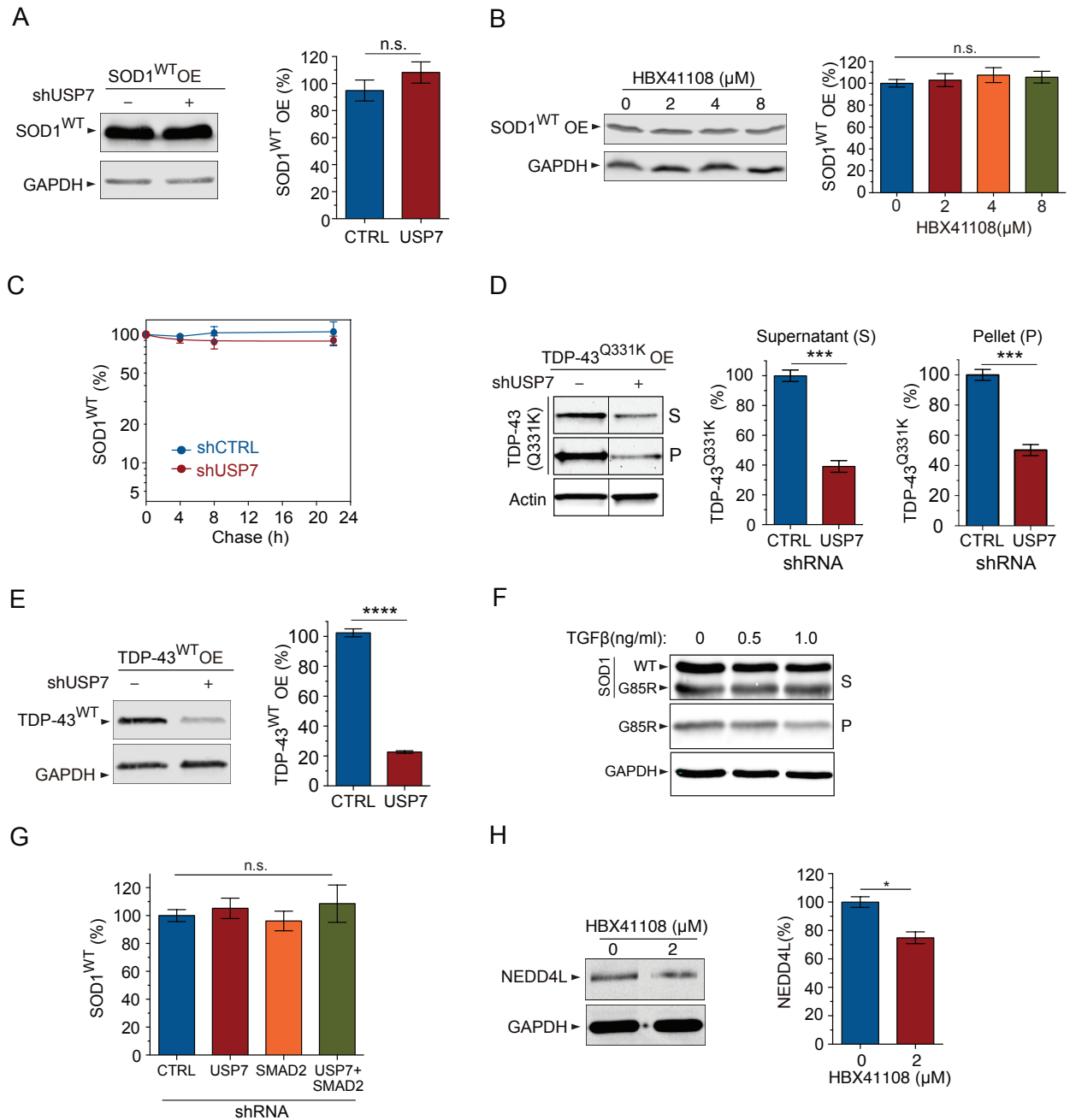
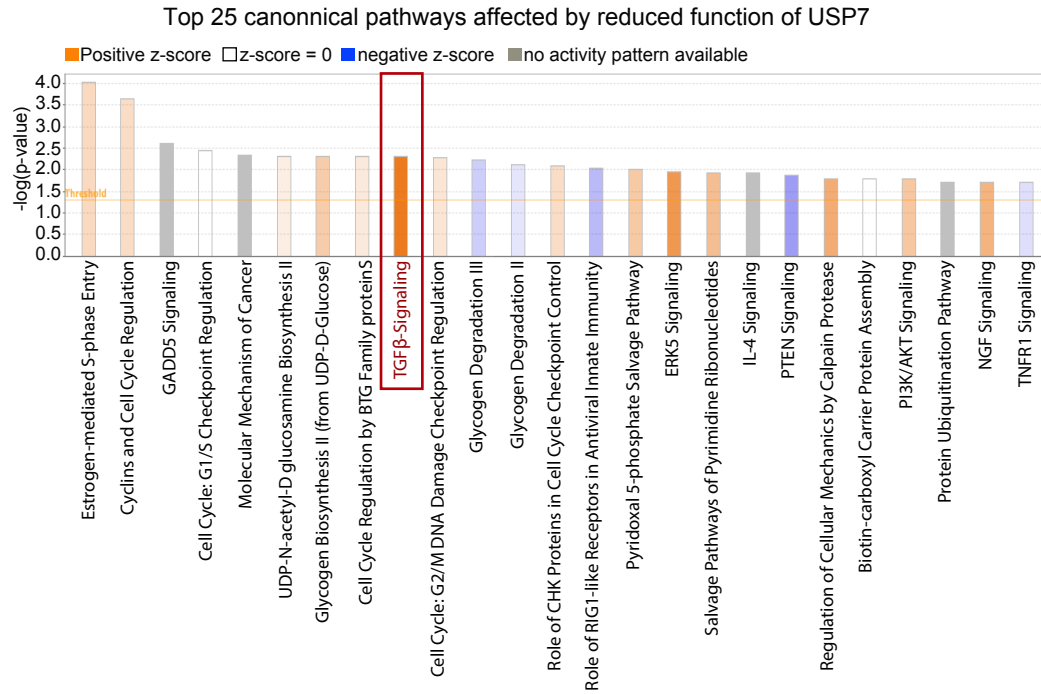


Fig. S2. The effects of loss of function of USP7 on the levels of different proteins. (A) Immunoblots of exogenous SOD1^{WT} protein in HEK293 cells after mock or USP7 knockdown (left). Quantification of SOD1^{WT} protein is shown (right; n=3, n.s., non-significant). (B) Immunoblots of exogenous SOD1^{WT} protein in HEK293 cells treated with increasing concentrations of HBX41108 (left). Quantification of SOD1^{WT} protein is shown (right; n=3, n.s.,

non-significant). (C) Quantification of endogenous SOD1^{WT} clearance after mock or USP7 knockdown in the cycloheximide chase experiments (**Fig. 2C**). The graph indicates the relative band intensity of SOD1^{WT} at each chase time point in the USP7 knockdown cells versus controls (n=3). (D) Immunoblot analysis of mutant TDP-43^{Q331K} proteins expressed in HEK293 cells after mock (CTRL) or USP7 knockdown (left). Quantification of both supernatant (S) and pellet (P) fractions is shown (right; n=3, *** $p < 0.001$). (E) Immunoblot analysis of exogenous TDP-43^{WT} proteins expressed in HEK293 cells after mock (CTRL) or USP7 knockdown (left). Quantification of TDP-43^{WT} protein is shown (right; n=3, **** $p < 0.0001$). (F) Treatment of cells with TGF β at the increasing concentrations led to a reduction in misfolded SOD1^{G85R} protein, but not SOD1^{WT} protein. (G) Quantification of Immunoblot analysis of SOD1^{WT} in HEK293 cells with USP7 or SMAD2 knockdown, or the double knockdown indicated that loss of USP7 or SMAD2 does not affect the protein level of SOD1^{WT} (n=4; n.s., non-significant). (H) Immunoblot analysis of endogenous NEDD4L in HEK293 cells treated with 2 μ M HBX41108 (left). Quantification of NEDD4L protein is shown (right; n=3, * $p < 0.05$). Error bars indicate \pm SEM.

Supplementary Figure 3

A



B

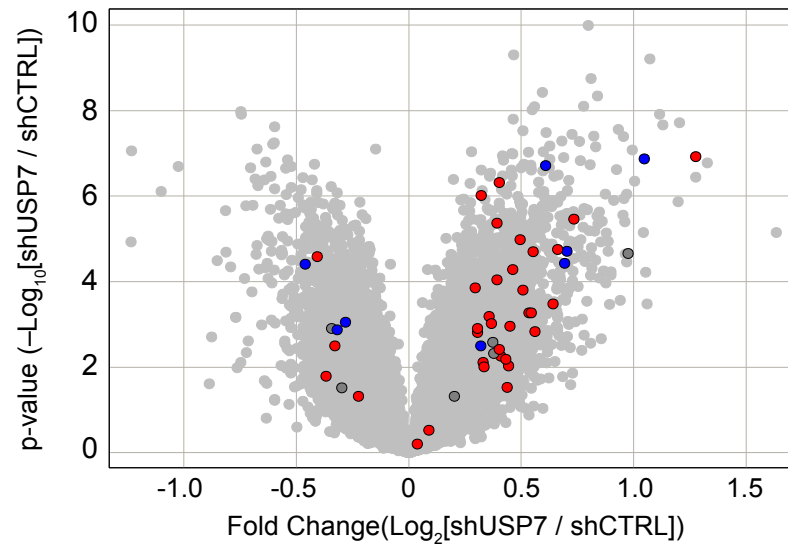
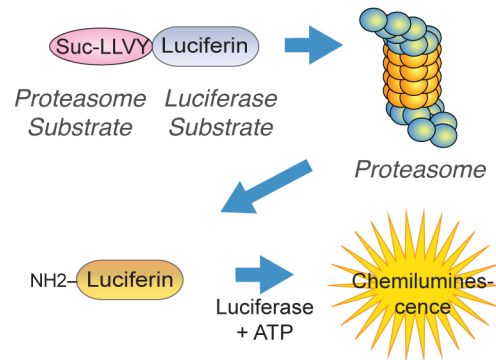


Fig. S3. Transcriptomic changes as a result of the loss of USP7. (A) Microarray analysis of transcriptomes of HEK293 cells with mock (CTRL) or USP7 knockdown. Among the top 25 canonical pathways identified by the Ingenuity Pathway Analysis software, TGF β signaling had

the best Z score ($Z = 5.07$) among the activated or inhibited pathways represented by the genes that are differentially regulated by the USP7 knockdown ($FC > 1.15$, $p < 0.1$). (B) The volcano scatter plot indicates -fold changes in the levels of gene transcripts affected differentially by the USP7 knockdown, as compared to the control. Gray spots represent >22,000 annotated transcripts. Red spots are predicted SMAD2-activated targets, and blue spots are predicted SMAD2-inhibited targets. The enrichment of red spots in the up-regulated genes and blue spots in the down-regulated genes indicates that the SMAD2-mediated transcription is activated by USP7 knockdown.

Supplementary Figure 4

A



B

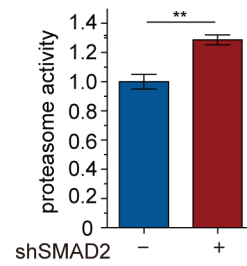
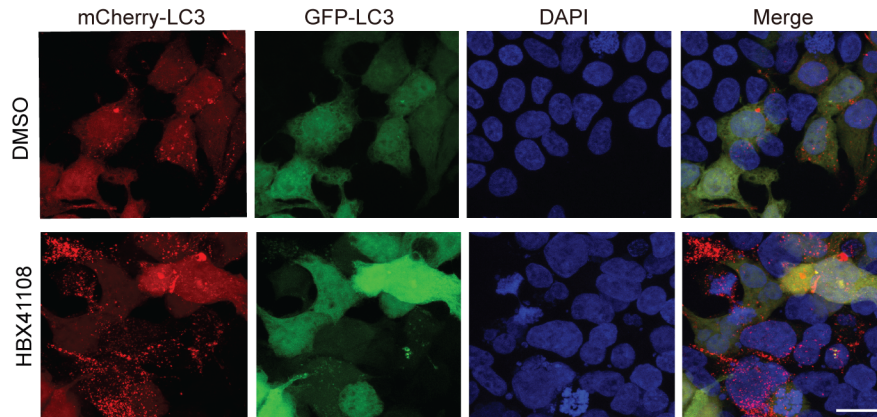


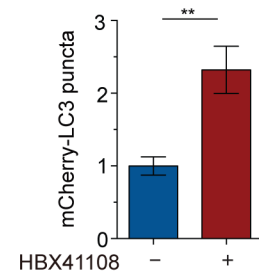
Fig. S4. SMAD2 negatively regulates proteasome activity. (A) Scheme of the proteasome activity assay workflow. (B) Proteasome activity of HEK293 cells after mock or SMAD2 knockdown. (n=3, ** $p < 0.01$). Error bars indicate \pm SEM.

Supplementary Figure 5

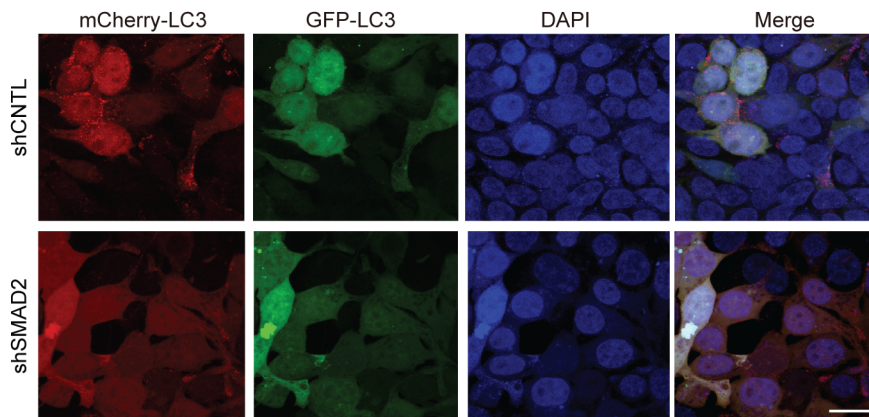
A



B



C



D

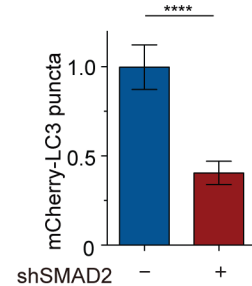


Fig. S5. Regulation of the autophagy flux as measured by a tandem fluorescent protein reporter. (A) Immunofluorescence of mCherry-GFP-LC3 in HEK293 cells after treatment with the USP7 inhibitor HBX41108. (B) Quantification of mCherry-LC3 puncta is shown (n=30; ** $p < 0.01$). (C) Immunofluorescence of mCherry-GFP-LC3 in HEK293 cells after mock or SMAD2 knockdown. (D) Quantification of mCherry-LC3 puncta is shown (n=30; **** $p < 0.0001$). Scale bar: 20 μm . Error bars indicate \pm SEM.

Supplementary Figure 6

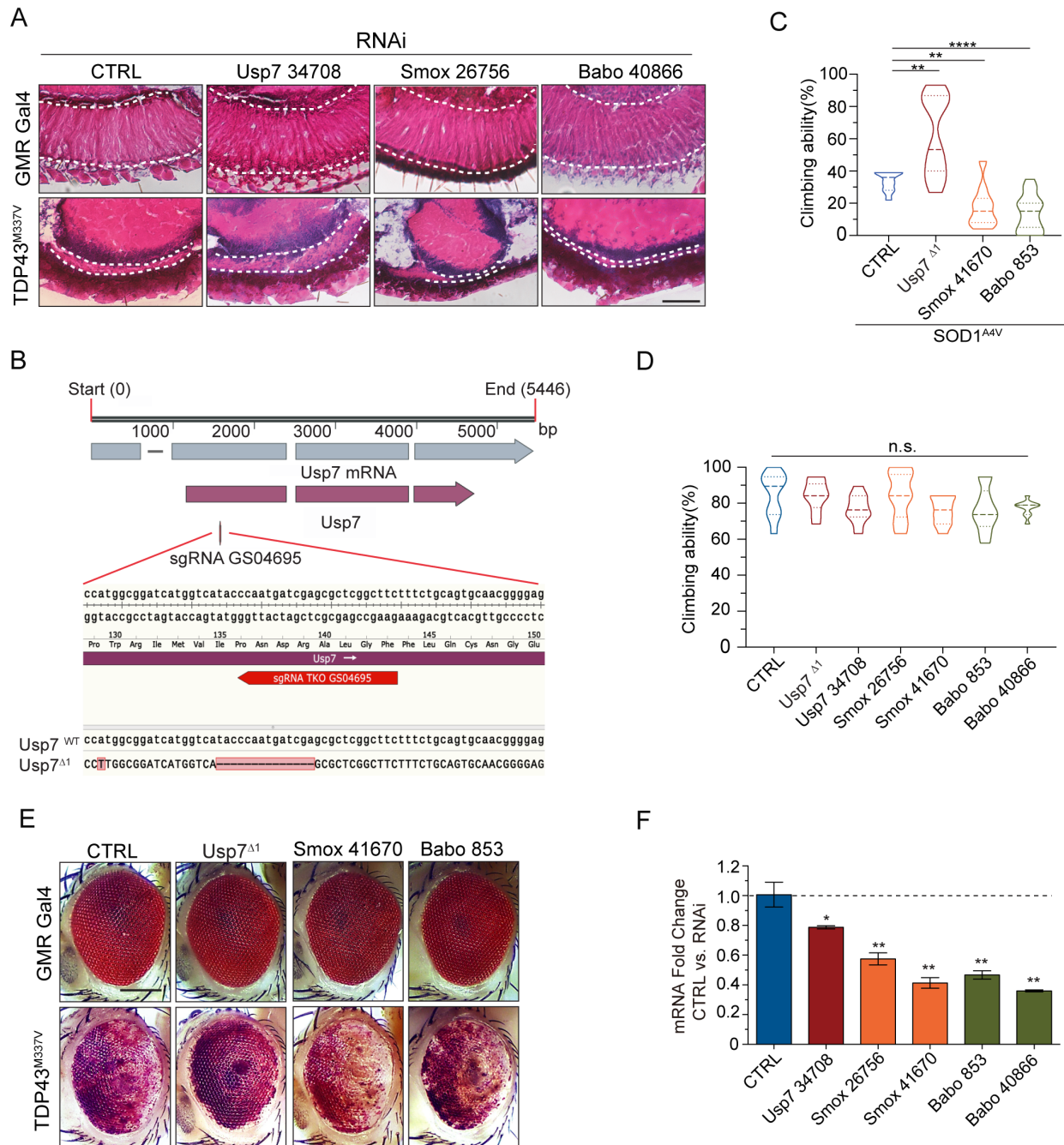


Fig. S6. The USP7-SMAD pathway modulates neurotoxicity induced by mutant SOD1 or TDP-43 in *Drosophila*. (A) H&E staining of eye tissue sections indicates that the reduction in Usp7 by RNAi (34708) strongly suppresses, while the reduction in Smox (RNAi 26756) or Babo (RNAi 40866) worsens, the eye degeneration phenotypes in TDP-43^{M337V} strains when

compared with the control Luc RNAi strain. The neuronal layer in the eye tissue is marked by white dotted lines. Scale bar: 50 μm . (B) Scheme of *Drosophila* Usp7 gene with the associated transcript and protein, and the position and sequence of the CRISPR-generated deletion allele Usp7 Δ^1 . The 14bp deletion is predicted to result in a translational frame shift and early termination of the polypeptide chain. (C) Quantification of the climbing ability of *Drosophila* expressing human SOD1^{A4V} in motor neurons, together with the heterozygous loss-of-function mutation Usp7 Δ^1 or gene-specific RNAi against Smox (RNAi 41670) or Babo (RNAi 853), or control RNAi, (n=8 independent groups; ** $p < 0.01$, **** $p < 0.0001$). (D) Quantification of the climbing ability of control *Drosophila* with the heterozygous loss-of-function mutation Usp7 Δ^1 or gene-specific RNAi against Smox (RNAi 41670) or Babo (RNAi 853), or control RNAi, in the presence of the *D42-GAL4* driver (n=8 independent groups; n.s., non-significant). (E) Reduction in Usp7 by the heterozygous loss-of-function mutation Usp7 Δ^1 strongly suppresses, while reduction in Smox (RNAi 41670) or Babo (RNAi 853) worsens, the eye degeneration phenotypes in TDP-43^{M337V} strains when compared with the control Luc RNAi strain. Scale bar: 100 μm . (F) Quantitative reverse transcription and PCR analysis indicates that the gene-specific RNAi is effective to reducing the respective mRNA levels (n=3; * $p < 0.05$, ** $p < 0.01$). Error bars indicate \pm SEM.

Supplementary Figure 7

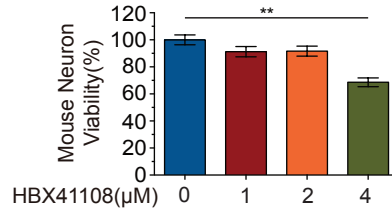


Fig. S7. Toxicity of USP7 inhibitor HBX41108 in mouse neurons. Quantification of mouse neuron survival with the treatment of increasing concentrations of HBX41108 (n=3; ** $p < 0.01$). Live cells were loaded with the calcein AM dye to determine the cell viability. Error bars indicate \pm SEM.

Supplementary Figure 8

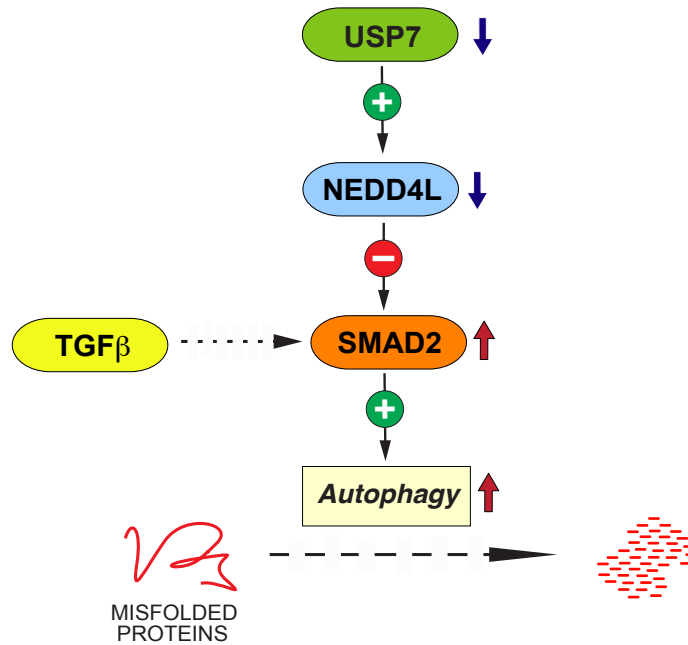


Fig. S8. A schematic model for the role of the USP7-SMAD2 pathway in the regulation of proteotoxicity. USP7 negatively regulates proteotoxicity through a pathway that is mediated by the SMAD2 activity. USP7 deubiquitinates NEDD4L and therefore positively regulates its levels. As the ubiquitin ligase of SMAD2, NEDD4L negatively regulates the level of SMAD2. As a result, loss of USP7 leads to the activation of SMAD2, which promotes autophagic activity to enhance the clearance of misfolded proteins.

Supplementary Table 1: List of genes whose RNAi inactivation leads to reduction of neuronal fluorescent reporter signal as well as other defects.

Gene	Sequence name	Phenotype*	Gene Function
eif-3.E	B0511.10	Gro	Translation initiation factor 3, subunit e (eIF-3e)
B0511.6	B0511.6	Gro	DEAD-box helicase 18
tag-264	B0511.8	Gro	mitochondrial ribosomal protein S30
nhr-23	C01H6.5	Gro	Nuclear Hormone Receptor-RAR related orphan receptor B/C
cel-1	C03D6.3	Gro	RNA guanylyltransferase and 5'-phosphatase
rpl-19	C09D4.5	Gro	60s ribosomal protein L19
let-502	C10H11.9	Let	Rho associated coiled-coil containing protein kinase 1/2
pab-3	C17E4.5	Gro	poly(A) binding protein nuclear 1
dcp-66	C26C6.5	Gro	GATA zinc finger domain containing 2A/2B
noah-1	C34G6.6	Gro	No mechanoreceptor potential A
pas-4	C36B1.4	Gro	proteasome 20S subunit alpha 7
prp-4	C36B1.5	Gro	pre-mRNA processing factor 4
cye-1	C37A2.4	Gro	G1/S-specific cyclin E
C43E11.9	C43E11.9	Gro	Ribosome biogenesis protein NIP7
C43H8.3	C43H8.3	Arrest (L2)	Uncharacterized protein
aspm-1	C45G3.1	Gro	Microtubule-associated protein Aspm
tba-2	C47B2.3	Gro	tubulin alpha 1a
pbs-2	C47B2.4	Gro	proteasome 20S subunit beta 7
C48B6.2	C48B6.2	Gro	IMP U3 small nucleolar ribonucleoprotein 3
C48B6.4	C48B6.4	Gro	Is predicted to have protein tyrosine phosphatase activity
C48E7.2	C48E7.2	Gro	RNA polymerase III (C) subunit
cyc-1	C54G4.8	Gro	Cytochrome c1
sulp-1	C55B7.6	Gro	sulfate permease family of anion transporters
rpl-24.1	D1007.12	Gro	ribosomal protein L24
rps-10	D1007.6	Gro	40s ribosomal protein s10
tsp-19	D2092.7	Gro	CD151 molecule (Raph blood group)); PRPH2 (peripherin 2); and TSPAN2 (tetraspanin 2)
let-504	E01A2.4	Emb, Protruding vulva	NFKB activating protein
asb-2	F02E8.1	Gro	ATP synthase peripheral stalk-membrane subunit b
rpl-11.2	F07D10.1	Gro	ribosomal protein L11
nmy-2	F20G4.3	Gro, Ste	myosin heavy chain 10
pdf-6	F21C3.5	Gro	Prefoldin subunit 6, KE2 family
rpa-0	F25H2.10	Gro	an acidic ribosomal subunit protein P0
pas-5	F25H2.9	Gro	proteasome 20S subunit alpha 5)
ncbp-2	F26A3.2	Gro	nuclear cap binding protein subunit 2
F26E4.6	F26E4.6	Gro	Cytochrome c oxidase, subunit VIIc/COX-7C
tba-1	F26E4.8	Gro	tubulin alpha 8-GTP binding activity
cco-1	F26E4.9	Gro	Cytochrome c oxidase, subunit 5B/COX5B
rab-5	F26H9.6	Gro	GTPase Rab5/YPT51 and related small G protein superfamily GTPases
atp-3	F27C1.7	Gro	ATP synthase peripheral stalk subunit OSCP
F30A10.10	F30A10.10	Gro	Ubiquitin carboxyl-terminal hydrolase
taf-5	F30F8.8	Gro, Ste	TATA-box binding protein associated factor 5
spd-2	F32H2.3	Gro	Uncharacterized protein, exhibits protein kinase binding activity
fasn-1	F32H2.5	Gro	Animal-type fatty acid synthase and related proteins
F32H2.8	F32H2.8	Gro	Uncharacterized protein of function DUF273
rps-15	F36A2.6	Gro	40S ribosomal protein S15
F36A2.7	F36A2.7	Gro	Uncharacterized protein
F37E3.1	F37E3.1	Gro	Nuclear cap-binding complex, subunit NCBP1/CBP80
rps-26	F39B2.6	Gro	ribosomal protein S26
tif-1	F39H11.2	Gro	TATA-box binding protein like 1
pbs-7	F39H11.5	Gro	proteasome 20S subunit beta 4
mfap-1	F43G9.10	Gro	Microfibrillar-associated protein MFAP1
F43G9.12	F43G9.12	Gro	PAX3 and PAX7 binding protein 1
vha-10	F46F11.5	Let	ATPase H+ transporting V1 subunit G2
rpl-25.2	F52B5.6	Gro	60s ribosomal protein L23
F53B6.4	F53B6.4	Gro	Uncharacterized protein, contains major sperm protein (MSP) domain
cct-3	F54A3.3	Gro	chaperonin containing TCP1 subunit 3
nath-10	F55A12.8	Gro	N-acetyltransferase 10
F55A3.7	F55A3.7	Gro	SPT16 homolog, facilitates chromatin remodeling subunit
npp-6	F56A3.3	Ste	nucleoporin 160
rpt-5	F56H1.4	Let	proteasome 26S subunit, ATPase 3
oac-35	F56H6.11	Gro, Emb	Uncharacterized protein, predicted to have transferase activity
let-607	F57B10.1	Let	cAMP responsive element binding protein 3
F58H10.1	F58H10.1	Gro	Uncharacterized protein
exos-3	F59C6.4	Gro	Exosomal 3'-5' exoribonuclease complex subunit Rrp40
F59C6.5	F59C6.5	Gro	NADH-ubiquinone oxidoreductase, subunit NDUFB10/PDSW

adr-1	H15N14.1	Let	adenosine deaminase domain containing 1
atp-1	H28O16.1	Gro	ATP synthase F1 subunit alpha
sec-12	K02B12.3	Gro	Prolactin regulatory element-binding protein/Protein transport protein SEC12p
tag-203	K02F2.3	Gro	Splicing factor 3b, subunit 3
ser-3	K02F2.6	Gro	octopamine receptor
his-40	K03A1.1	Gro	Histone H3C1
eif-2beta	K04G2.1	Gro	Translation initiation factor 2, beta subunit (eIF-2beta)
pbs-5	K05C4.1	Gro	20S proteasome, regulatory subunit beta type PSMB5/PSMB8/PRE2
knl-2	K06A5.4	Sick	MIS18 binding protein 1
cdc-25.1	K06A5.7	Sick	cell division cycle 25A/B/C
hsp-2	K09C4.3	Gro	hsp-2 Pseudogene
spc-1	K10B3.10	Egl	Ca2+-binding actin-bundling protein (spectrin), alpha chain (EF-Hand protein superfamily)
ran-4	R05D11.3	Gro	Nuclear transport factor 2
imb-2	R06A4.4	Gro	transportin 1/2
adsl-1	R06C7.5	Gro	Adenylosuccinate lyase
rpn-8	R12E2.3	Sick (severe)	proteasome 26S subunit, non-ATPase 7
T04G9.4	T04G9.4	Gro	Alpha-aminoacidic semialdehyde dehydrogenase-phosphopantetheinyl transferase
rps-17	T08B2.10	Gro	40S ribosomal protein S17
T08B2.7	T08B2.7	Gro	Hydroxyacyl-CoA dehydrogenase/enoyl-CoA hydratase
T08G11.4	T08G11.4	Gro	trimethylguanosine synthase 1
T09B4.9	T09B4.9	Gro	translocase of inner mitochondrial membrane 44
his-4	T10C6.11	Gro	Histone H2B
his-3	T10C6.12	Gro	Histone 2A
glh-4	T12F5.3	Gro	exhibits JUN kinase binding activity
vha-15	T14F9.1	Gro	ATPase H+ transporting V1 subunit H
ngp-1	T19A6.2	Gro, Ste	G protein nucleolar 2
T21G5.2	T21G5.2	Gro	localize to integral component of membrane
T21G5.4	T21G5.4	Gro	Sperm Meiosis PDZ domain containing proteins
mup-2	T22E5.5	Gro	Troponin
his-67	T23D8.5	Gro	H4 clustered histone 2
his-68	T23D8.6	Gro	H2A.X variant histone
T25G3.3	T25G3.3	Gro	NMD3 ribosome export adaptor
pri-2	W02D9.1	Gro	DNA primase subunit 2
W03D8.4	W03D8.4	Gro	Uncharacterized protein
W04A8.2	W04A8.2	Gro	Uncharacterized protein
lpr-3	W04G3.8	Gro	Uncharacterized protein, predicated containing Calycin domain
rps-20	Y105E8A.16	Gro	40S ribosomal protein S20
apg-1	Y105E8C.n	Gro	adaptor related protein complex 1 subunit gamma 1
pab-1	Y106G6H.2	Gro	poly(A) binding protein cytoplasmic 1
rpl-30	Y106G6H.3	Gro	ribosomal protein L30
Y110A7A.11	Y110A7A.11	Gro	Vesicle transport protein USE1
Y110A7A.8	Y110A7A.8	Gro (severe)	pre-mRNA processing factor 31
icp-1	Y39G10AR.13	Gro	AFG3 like matrix AAA peptidase subunit 2
mcm-4	Y39G10AR.14	Gro	minichromosome maintenance complex component 4
klp-19	Y43F4B.6	Emb	kinesin family member 4A
spg-7	Y47G6A_247.g	Gro	AFG3 like matrix AAA peptidase subunit 2
imb-5	Y48G1A.5	Gro	Nuclear export receptor CSE1/CAS (chromosome segregation 1 like)
rpl-17	Y48G8AL.8	Gro	60S ribosomal protein L22
grh-1	Y48G8AR.1	Emb	grainyhead like transcription factor 1
Y54E10BR.6	Y54E10B_159.c	Gro	DNA-directed RNA polymerase II subunit RPB7
tfg-1	Y63D3A.5	Gro	TFG(trafficking from ER to golgi regulator)
Y65B4BR.5	Y65B4B_10.d	Gro	Transcription factor containing NAC and TS-N domains
Y65B4BL.2	Y65B4BL.2	Gro	deps-1 (DEfective P granules and Sterile)
Y71A12B.a	Y71A12B.a	Gro	Uncharacterized protein
rpl-1	Y71F9AL.13	Gro	RPL10A (ribosomal protein L10a)
snr-7	Y71F9B.4	Gro	Small Nuclear ribonucleoprotein G
lsm-6	Y71G12A_187.b	Emb	Small nuclear ribonucleoprotein F
Y71G12B.11	Y71G12B.11	Gro, Dmp	Talin2
rps-7	ZC434.2	Gro	40S ribosomal protein S7
nol-16	ZK265.6	Gro	NOP16 nucleolar protein

*Abbreviations for phenotypic descriptions

Gro	abnormal growth
Let	lethal
Emb	embryonic lethality
Ste	sterile
Dmp	dumpy

Supplementary Table 2: List of patients' tissues.

Sample No.	Patient ID	Source	Clinical diagnosis	ALS pathology	Age of sampling	Gender	Region
1	90015	VABBB	CTRL	Non	66	M	SC-C
2	90018	VABBB	CTRL	Non	82	M	SC-C
3	100012	VABBB	CTRL	Non	81	F	SC-C
4	120016	VABBB	CTRL	Non	63	F	SC-C
5	95	JHMI	CTRL	Non	72	M	SC-C
6	103	JHMI	CTRL	Non	22	M	SC-C
7	110	JHMI	CTRL	Non	50	M	SC-C
8	108	JHMI	CTRL	Non	72	M	SC-C
9	100007	VABBB	fALS-C9orf72	Yes (TDP-43 positive)	61	M	SC-C
10	100040	VABBB	ALS	Yes	88	M	SC-C
11	120015	VABBB	ALS	Yes (TDP-43 positive)	58	M	SC-C
12	38	JHMI	sALS-C9orf72	Yes	34	F	SC-C
13	88	JHMI	fALS-C9orf72, FTD	Yes	59	M	SC-C
14	92	JHMI	fALS-C9orf72	Yes	72	M	SC-C
15	NEUTP019MY9	BNI	ALS-C9orf72	Yes	62	F	SC-C
16	90003	VABBB	fALS	Yes	73	M	SC-C
17	90005	VABBB	ALS	Yes	65	M	SC-C
18	90020	VABBB	fALS-SOD1 L145F	Yes	49	F	SC-C
19	100002	VABBB	ALS	Yes	63	M	SC-C
20	110011	VABBB	ALS	Yes (TDP-43 positive)	83	M	SC-C
21	130014	VABBB	ALS	Yes (TDP-43 positive)	70	M	SC-C
22	130020	VABBB	ALS	Yes (TDP-43 positive)	78	M	SC-C
23	130022	VABBB	ALS	Yes (TDP-43 positive)	48	M	SC-C
24	130025	VABBB	ALS	Yes (TDP-43 positive)	77	M	SC-C
25	140008	VABBB	ALS	Yes (TDP-43 positive)	75	M	SC-C
26	AZ140006	VABBB	ALS	Yes (TDP-43 positive)	74	M	SC-C
27	AZ140017	VABBB	ALS	Yes (TDP-43 positive)	66	M	SC-C

28	AZ140021	VABBB	ALS	Yes	63	M	SC-C
29	AZ140023	VABBB	ALS	Yes (TDP-43 positive)	68	M	SC-C
30	AZ150001	VABBB	ALS	Yes (TDP-43 positive)	65	M	SC-C
31	AZ150004	VABBB	ALS	Yes (TDP-43 positive)	67	M	SC-C
32	AZ160030	VABBB	ALS	Yes (TDP-43 positive)	65	M	SC-C

Abbreviations: ALS (Amyotrophic Lateral Sclerosis), fALS (Familial Amyotrophic Lateral Sclerosis), sALS (Sporadic Amyotrophic Lateral Sclerosis), FTD (Frontotemporal Dementia), CTRL (Control), M (Male), F (Female), N/A (Not Applicable), JHMI (Johns Hopkins Medical Institute), VABBB (VA Biorepository Brain Bank), BNI (Barrow Neurological Insititute), SC-C (Spinal Cord-Cervical). The mean age of the controls is 63.5 years versus 65.9 years for the patients.